

## ROBOT PARAMETER IDENTIFICATION AND REDUNDANCY ANALYSIS BASED ON ADAPTIVE RIDGE REGRESSION

by

**Yonggang KANG\***, **Guomao LI**, **Shuaijia KOU\***, **Wentao YU**,  
**Siren SONG**, and **Zihao WANG**

School of Mechanical Engineering, Northwestern Polytechnical University, Xi'an, China

Original scientific paper  
<https://doi.org/10.2298/TSCI2503095K>

*This paper proposes an iterative parameter identification algorithm based on adaptive ridge regression to establish a geometric error model for improving the absolute positioning accuracy of the end-effector of collaborative robots. The perturbation method is employed to establish the aforementioned model. This algorithm addresses the overfitting and lack of regularization issues associated with the least squares method under multicollinearity and high-dimensional data, thereby enhancing the model generalization capability. A parameter redundancy analysis was conducted on the positional error model for multi-degree-of-freedom collaborative robots. The experimental results demonstrate that the elimination of redundant parameters through analytical methods improves the reliability and accuracy of parameter identification and enhances the model robustness. In comparison to the least squares method, the proposed algorithm demonstrates superior identification accuracy and generalization capability, resulting in a notable enhancement in the absolute positioning accuracy of collaborative robots through calibration.*

Key words: *kinematic calibration, parameter identification, error compensation, parameter redundancy*

### Introduction

Collaborative robots are commonly utilized in industrial production and automated processing due to their inherent safety, efficiency, and flexibility, particularly in contexts that necessitate high flexibility, low production volumes, and diverse product types. The integration of human and robotic elements within a collaborative framework has the potential to enhance the quality and comfort of the work environment, while simultaneously addressing the demands for low-cost, high-efficiency, and complex task automation [1, 2]. It is of paramount importance to calibrate the robot in order to enhance the precision of its absolute positioning capabilities [3]. However, deviations between actual and theoretical parameters are introduced as a result of machining errors, assembly errors, and wear, which in turn reduce end-effector pose accuracy. Geometric parameter errors account for 90% of the total error [4, 5], making their calibration essential for positioning accuracy.

The calibration of geometric parameters based on robot kinematics comprises four stages: the establishment of the calibration model, the measurement stage, the parameter iden-

\* Corresponding authors, e-mail: kangyonggang@nwpu.edu.cn; koushuaijia@mail.nwpu.edu.cn

tification stage, and the compensation stage [6]. The Denavit-Hartenberg (DH) model is a widely utilized approach for kinematic modeling, facilitating the acquisition of transformation matrices through homogeneous transformations [7, 8]. However, the DH model is not without its limitations, particularly when adjacent joints are parallel, which can result in singularities. The MDH model addresses this issue by incorporating a rotation parameter around the  $Y$ -axis [9]. The CPC and product of exponentials models have also been developed, but they are complex and involve a considerable number of parameters [10, 11]. Common measurement methods include open-loop and closed-loop approaches employing laser measurement devices, co-ordinate measuring machines, and laser scanners [12-14]. Linear methods, such as the least squares method, are susceptible to matrix singularity and the presence of redundant parameters [15, 16]. Non-linear optimization methods, on the other hand, can be complex and prone to local optima [17, 18].

This paper puts forth a methodology for the identification of parameters and the elimination of redundancy in multi-DoF robots. The method employs cross-validation to automatically identify the optimal regularization parameter, addressing stability and overfitting issues in least squares identification and enhancing model generalizability. An analytical method for redundant parameters, including end-effector tools, ensures accuracy and robustness. The efficacy of the proposed method is corroborated by the experimental results.

## Establishment of the robotic geometric model

### *Kinematic modeling of robots*

This paper employs an improved MDH modeling method, effectively resolving the singularity issues that arise in the DH model when adjacent joints are parallel [9]. Thus, the homogeneous co-ordinate transformation matrix for adjacent joints of the robot is:

$${}^{i-1}\mathbf{T} = \mathbf{Rot}_x(\alpha_{i-1})\mathbf{Trans}_x(a_{i-1})\mathbf{Rot}_z(\theta_i)\mathbf{Trans}_z(d_i)\mathbf{Rot}_y(\beta_i) \quad (1)$$

where  $\alpha_{i-1}$ ,  $d_i$ ,  $a_{i-1}$ ,  $\theta_i$  are the link twist angle, link offset, link length, and joint angle, respectively, and  $\beta_i$  – the rotational transformation around the axis.

For an  $N$ -DoF serial robot, the product of the transformations of each adjacent link yields the transformation matrix between the base co-ordinate system and the end-effector co-ordinate system of the robotic arm.

$${}^0\mathbf{T}_N = {}^0\mathbf{T}_1\mathbf{T}_2\mathbf{T}_3\cdots\mathbf{T}_N = \begin{bmatrix} {}^0\mathbf{R}_N & {}^0\mathbf{P}_N \\ \mathbf{0} & 1 \end{bmatrix} \quad (2)$$

where  ${}^0\mathbf{R}_N$  is the rotation matrix and  ${}^0\mathbf{P}_N$  is the position component.

### *Error modeling of robots*

It is inevitable that robots will exhibit both geometric and non-geometric errors during manufacturing, which will result in deviations between the end-effector pose and the commanded pose. Empirical evidence suggests that over 90% of these errors are geometric in nature [19, 20]. In practical calibration, the measurement of pose requires the use of high-end equipment, whereas the measurement of position is relatively straightforward. Given the strong coupling between position accuracy and pose accuracy, improvements in position accuracy will also enhance pose accuracy. Accordingly, this paper is dedicated to an in-depth examination of positional inaccuracies. A robot position error model is established using the

perturbation method, wherein pose deviations are viewed as results of small translations and rotations through differential transformation. The model construction is illustrated in fig. 1.

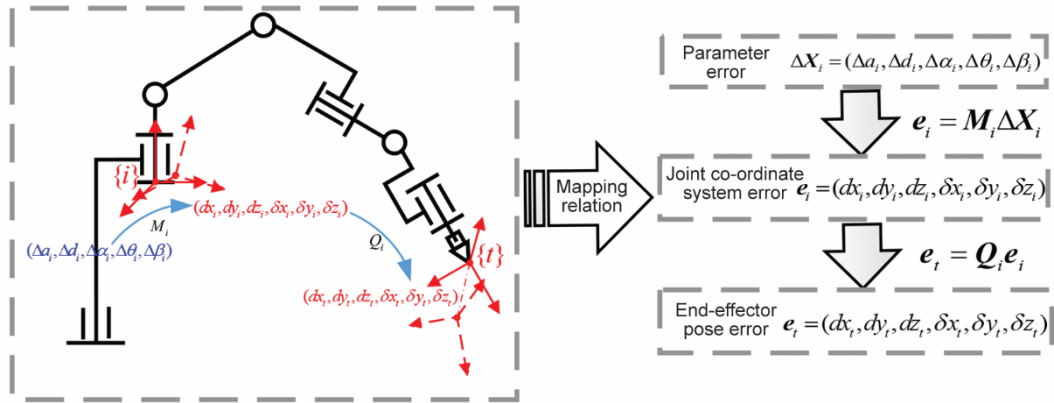


Figure 1. Perturbation method error model modeling approach

Using  $\Delta a_{i-1}, \Delta d_i, \Delta \alpha_{i-1}, \Delta \theta_i, \Delta \beta_i$  to represent the geometric parameter errors of the links, the actual pose transformation matrix is expressed as:

$${}^{i-1}T^R = \mathbf{Rot}_x(\alpha_{i-1} + \Delta \alpha_{i-1}) \mathbf{Trans}_x(a_{i-1} + \Delta a_{i-1}) \mathbf{Rot}_z(\theta_i + \Delta \theta_i) \mathbf{Trans}_z(d_i + \Delta d_i) \mathbf{Rot}_y(\beta_i + \Delta \beta_i) \quad (3)$$

Therefore, the pose transformation error at link  $i$  is:

$$d_i^{i-1}T_i = {}^{i-1}T^R {}_i^{i-1}T = {}_i^{i-1}T \Delta_i \quad (4)$$

Taking the total differential of each MDH parameter in eq. (1) yields:

$$d_i^{i-1}T_i = \frac{\partial {}_i^{i-1}T}{\partial a_{i-1}} \Delta a_{i-1} + \frac{\partial {}_i^{i-1}T}{\partial d_i} \Delta d_i + \frac{\partial {}_i^{i-1}T}{\partial \alpha_{i-1}} \Delta \alpha_{i-1} + \frac{\partial {}_i^{i-1}T}{\partial \theta_i} \Delta \theta_i + \frac{\partial {}_i^{i-1}T}{\partial \beta_i} \Delta \beta_i \quad (5)$$

By combining eqs. (4) and (5):

$$\Delta_i = ({}_i^{i-1}T)^{-1} d_i^{i-1}T = \begin{bmatrix} S[\delta_i] & d_i \\ \mathbf{0} & 0 \end{bmatrix} \quad (6)$$

where  $\delta_i$  and  $d_i$  represent the differential translation and rotational motion vectors, respectively, and  $S[\delta_i]$  is the antisymmetric matrix with respect to  $\delta_i$ . This definition will be used throughout the following text.

Arranging the terms of eq. (6) into the vector form of differential motion yields:

$$\mathbf{e}_i = \begin{bmatrix} dx_i \\ dy_i \\ dz_i \\ \delta x_i \\ \delta y_i \\ \delta z_i \end{bmatrix} = \begin{bmatrix} c\beta_i c\theta_i & -s\beta_i & -d_i c\beta_i s\theta_i & 0 & 0 \\ -s\theta_i & 0 & -d_i c\theta_i & 0 & 0 \\ s\beta_i c\theta_i & c\beta_i & -d_i s\beta_i s\theta_i & 0 & 0 \\ 0 & 0 & c\beta_i c\theta_i & -s\beta_i & 0 \\ 0 & 0 & -s\theta_i & 0 & 1 \\ 0 & 0 & s\beta_i c\theta_i & c\beta_i & 0 \end{bmatrix} \begin{bmatrix} \Delta\alpha_{i-1} \\ \Delta d_i \\ \Delta\alpha_{i-1} \\ \Delta\theta_i \\ \Delta\beta_i \end{bmatrix} = \mathbf{M}_i \Delta \mathbf{X}_i \quad (7)$$

where  $\mathbf{M}_i = [\mathbf{M}_{\alpha_{i-1}} \quad \mathbf{M}_{d_i} \quad \mathbf{M}_{\alpha_{i-1}} \quad \mathbf{M}_{\theta_i} \quad \mathbf{M}_{\beta_i}]$ , and  $\mathbf{e}_i$  represent the pose error vector of the joint co-ordinate system caused by the geometric parameter error  $\Delta \mathbf{X}_i$ .

Due to inevitable errors introduced during the installation and manufacturing of the end-effector tool, the impact of tool parameter errors needs to be considered. It is usually stipulated that the pose of the end-effector tool co-ordinate system aligns with the robot flange co-ordinate system, *i.e.*, the rotation matrix  ${}^N_t \mathbf{R} = \mathbf{I}$ . Let  ${}^N_t \mathbf{P} = [x_t \ y_t \ z_t \ rx_t \ ry_t \ rz_t]$ , similar to the derivation in eq. (7), be:

$$\mathbf{e}_t = \mathbf{M}_t \Delta \mathbf{X}_t = \Delta \mathbf{X}_t \quad (8)$$

According to the principle of robot differential transformation [21], the same differential motion in different reference co-ordinate systems is represented as  $\Delta_t = ({}^i_t \mathbf{T})^{-1} \cdot \Delta_i \cdot {}^i_t \mathbf{T}$ . Arranging the  $\Delta_i$  terms into the vector form of differential motion yields:

$${}^t \mathbf{e}_i = \begin{bmatrix} {}^t d_i \\ {}^t \delta_i \end{bmatrix} = \begin{bmatrix} {}^t \mathbf{R} & -{}^t \mathbf{R} \mathbf{S} [{}^i_t \mathbf{P}] \\ \mathbf{0} & {}^t \mathbf{R} \end{bmatrix} \begin{bmatrix} d_i \\ \delta_i \end{bmatrix} \quad (9)$$

where  ${}^t \mathbf{e}_i$  represents the differential motion caused by the parameter error of the  $i^{\text{th}}$  link, propagated to the end-effector co-ordinate system.

Therefore, the robot position error model is described as:

$$\mathbf{e}_p = \begin{bmatrix} {}^0_t \mathbf{R} & \mathbf{0} \end{bmatrix} {}^t \mathbf{e} = \sum_{i=1}^{1,2,\dots,N,t} \begin{bmatrix} {}^0_t \mathbf{R} & -{}^0_t \mathbf{R} \mathbf{S} [{}^i_t \mathbf{P}] \end{bmatrix} \mathbf{M}_i \Delta \mathbf{X}_i = \sum_{i=1}^{1,2,\dots,N,t} {}^p \mathbf{J}_i \Delta \mathbf{X}_i \quad (10)$$

where  ${}^p \mathbf{J}_i$  represents the position identification Jacobian matrix of the robotic arm.

## Redundancy analysis and parameter identification

### Analysis of parameter redundancy

When the error model contains a substantial number of superfluous parameters, the identification Jacobian matrix becomes non-full rank, thereby causing the condition number of the equation to approach infinity. Consequently, it is of paramount importance to conduct a redundancy analysis of the error model and eliminate any redundant parameters in order to enhance the accuracy and robustness of parameter identification. Starting with the configuration of the identification Jacobian matrix, analyzing eq. (10) by substituting  $\mathbf{M}_i$ ,  $\mathbf{M}_t$ , and the nominal value  $\beta_i = 0$ , the coefficient arrays are:

$${}^P\mathbf{J}_{\alpha_{i-1}} = {}^0\mathbf{R} [c\theta_i \quad -s\theta_i \quad 0]^T, \quad {}^P\mathbf{J}_{d_i} = {}^0\mathbf{R} [0 \quad 0 \quad 1]^T, \quad {}^P\mathbf{J}_{\theta_i} = -{}^0\mathbf{R} \begin{bmatrix} {}^iP_y & -{}^iP_x & 0 \end{bmatrix}^T$$

$${}^P\mathbf{J}_{\alpha_{i-1}} = {}^0\mathbf{R} \begin{bmatrix} -d_i s\theta_i & -{}^iP_z s\theta_i & -d_i c\theta_i & -{}^iP_z c\theta_i & {}^iP_y c\theta_i & +{}^iP_x s\theta_i \end{bmatrix}^T, \quad (11)$$

$${}^P\mathbf{J}_{\beta_i} = -{}^0\mathbf{R} \begin{bmatrix} -{}^iP_z & 0 & {}^iP_x \end{bmatrix}^T$$

$$\begin{bmatrix} {}^P\mathbf{J}_{x_i} & {}^P\mathbf{J}_{y_i} & {}^P\mathbf{J}_{z_i} \end{bmatrix} = {}^0\mathbf{R} \mathbf{I}, \quad {}^P\mathbf{J}_{rx_i} = {}^P\mathbf{J}_{ry_i} = {}^P\mathbf{J}_{rz_i} = \mathbf{0} \quad (12)$$

In the case of serial robots, an analysis of the identification Jacobian matrix of adjacent joint co-ordinate systems is sufficient to identify all redundant parameters. It is thus necessary to analyse the redundancy between both similar and different types of parameters. The properties of rotation matrix multiplication and invertibility are employed to rewrite the identification arrays of adjacent links, eliminating equal parts, resulting in a linearly related array for the MDH error model that includes tool parameters. The linear related arrays and their corresponding redundant parameters are summarized in tab. 1.

**Table 1. The MDH error redundant parameter table with tool parameters**

	Constraints	Linear relationships	Redundant parameters
Measure position	None	${}^P\mathbf{J}_{rx_i} = {}^P\mathbf{J}_{ry_i} = {}^P\mathbf{J}_{rz_i} = \mathbf{0}$ ${}^P\mathbf{J}_{z_i} = {}^P\mathbf{J}_{d_N}$	$\Delta rx_i, \Delta ry_i, \Delta rz_i$ $\Delta z_i$ or $\Delta d_N$
	$\alpha_{i-1} = 0$ or $\alpha_{i-1} = 180^\circ$	${}^P\mathbf{J}_{d_i} = \pm {}^P\mathbf{J}_{d_{i-1}}$	$\Delta d_i$
	$\alpha_{N-2} = \pm 90^\circ$ and $a_{N-2} = 0$	${}^P\mathbf{J}_{\theta_{N-1}} = \mp {}^P\mathbf{J}_{\beta_{N-2}}$	$\Delta \theta_{N-1}$ or $\Delta \beta_{N-2}$
	$x_i = y_i = 0$	${}^P\mathbf{J}_{\theta_N} = \mathbf{0}$	$\Delta \theta_N$
	$x_i = y_i = 0$ and $\alpha_{N-1} = \pm 90^\circ$	${}^P\mathbf{J}_{\alpha_{N-1}} = \mp (d_N + z_i) {}^P\mathbf{J}_{d_{N-1}}$	$\Delta \alpha_{N-1}$ or $\Delta d_{N-1}$
	$x_i = y_i = 0$ and $\alpha_{N-1} = \pm 90^\circ$ , $a_{N-1} = 0$	${}^P\mathbf{J}_{\theta_{N-1}} = \pm (d_N + z_i) {}^P\mathbf{J}_{\alpha_{N-1}}$	$\Delta \theta_{N-1}$ or $\Delta d_{N-1}$

*Iterative parameter identification based on adaptive ridge regression*

At present, the most frequently employed methodology for parameter identification is the least squares method [22, 23]. This method is relatively straightforward and efficient, but its effectiveness is contingent upon the initial values selected. If these values are not optimal, the method may result in local convergence, potentially influencing the identification outcomes. Furthermore, the method is susceptible to issues when confronted with multicollinearity and high-dimensional data, which can easily result in overfitting. To address these issues, this paper proposes an adaptive ridge regression iterative algorithm for robot geometric parameter identification. The algorithm selects the optimal regularization parameter through cross-validation, combining the regularization properties of ridge regression with the model evaluation capabilities of cross-validation to improve generalization performance and prevent overfitting.

$$\min_{\Delta X} (\|\mathbf{J} \Delta X - \mathbf{e}\|^2 + \lambda \|\Delta X\|^2) \quad (13)$$

where  $\lambda \|\Delta X\|^2$  is the regularization term and  $\lambda$  is the regularization parameter.

To select the optimal  $\lambda$ , cross-validation is used for evaluation. This paper employs  $k$ -fold cross-validation, which includes four steps: partitioning subsets, training and validation, calculating the performance metric for  $k$ -fold cross-validation, and selecting the regularization parameter with the best performance. The entire iterative process for robot parameter identification is shown in fig. 2.

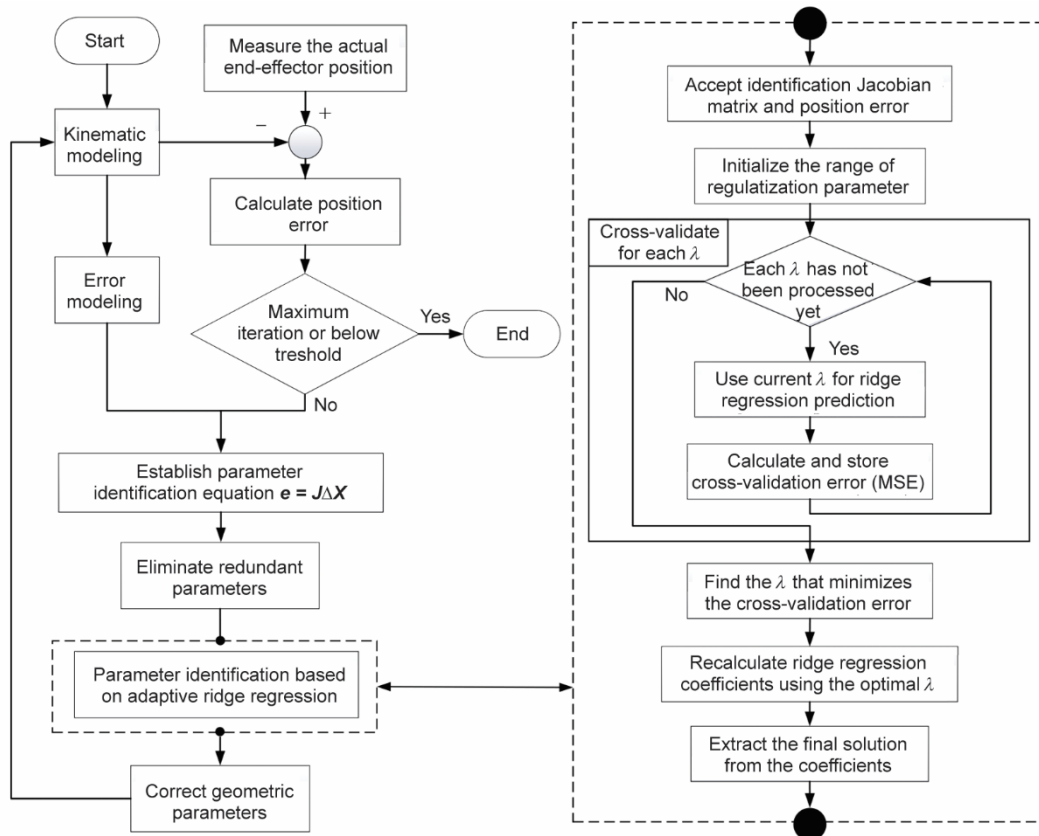


Figure 2. Flowchart of iterative parameter identification based on adaptive ridge regression

### Experiment and results analysis

The six-DoF collaborative robot JAKA ZU18 is used as the research object in this paper to validate the described redundancy parameter elimination and iterative parameter identification algorithm. The nominal geometric parameters of the collaborative robot are shown in tab. 2.

Referencing tabs. 1 and 2, redundancy analysis of the model indicates that the redundant parameter  $\Delta r_{x_i}, \Delta r_{y_i}, \Delta r_{z_i}, \Delta z_i, \Delta d_3, \Delta d_4, \Delta \alpha_5, \Delta a_5, \Delta \theta_5, \Delta \theta_6$  needs to be eliminated. The number of error parameters to be identified decreases from 32 to 22.

To validate the effectiveness of the robot error model, the elimination of redundant parameters, and the performance of the proposed iterative parameter identification algorithm, the following experiment was designed:

- Preset the geometric parameter errors of the collaborative robot according to the error model.

- Based on the joint angle range in tab. 2, randomly sample 40 sets of joint angles that meet the error model identification conditions  $n \geq k/3$ .
- Substitute the nominal geometric parameters and joint angle samples from tab. 2 into the kinematic model to calculate the nominal end-effector positions. Then, modify the nominal geometric parameters using the preset geometric errors as the actual geometric parameters to calculate the actual positioning positions.
- Perform iterative identification of geometric parameter errors using both the least squares method and the adaptive ridge regression iterative algorithm. Consider two scenarios: one including all error parameters and the other excluding redundant parameters. Use the identification results to correct the kinematic model, then randomly select 20 spatial measurement points to calculate the positioning error after geometric parameter calibration to assess the accuracy of the algorithms.

**Table 2. Nominal geometric parameters of the collaborative robot**

Joint number	$a_{i-1}$ [mm]	$d_i$ [mm]	$\alpha_{i-1}$ [°]	$\theta_i$ [°]	$\beta_i$ [°]	Joint range [°]
1	0	142.65	0	$\theta_1$	-	-360~360
2	0	-181.65	90	$\theta_2$	-	-85~265
3	510	0	0	$\theta_3$	0	-175~175
4	400	27.65	0	$\theta_4$	0	-85~265
5	0	115	90	$\theta_5$	-	-360~360
6	0	103.5	-90	$\theta_6$	-	-360~360
$t$	$x_t = 0, y_t = 0, z_t = 15$			$rx_t = 0, ry_t = 0, rz_t = 0$		

Using the least squares method, perform identification and calibration for both cases: one with all error parameters and one with redundant parameters removed, as shown in figs. 3 and 4. The results of iterative identification and calibration using the adaptive ridge regression algorithm are shown in figs. 5 and 6, and tab. 3.

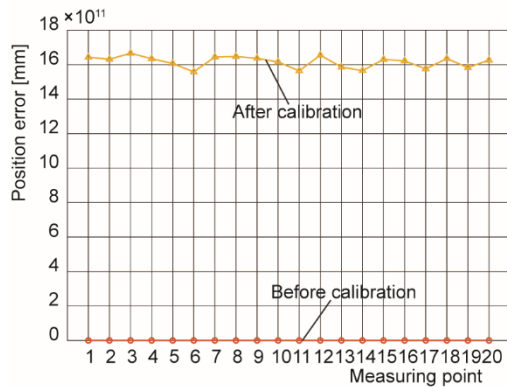


**Figure 3. Least squares calibration results with all parameters**

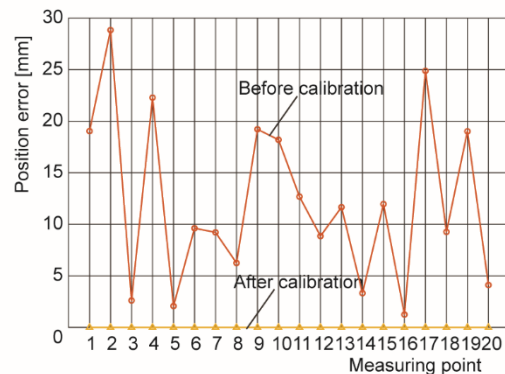


**Figure 4. Least squares calibration results with redundant parameters removed**

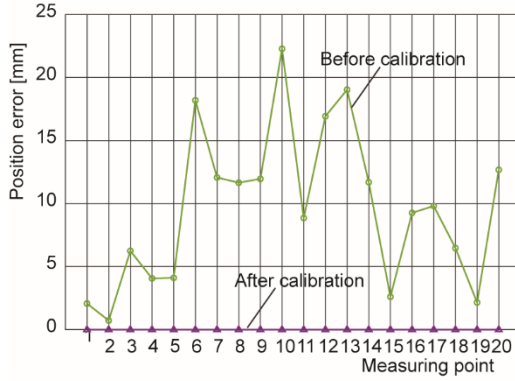


Figure 5. Adaptive ridge regression calibration results including all parameters

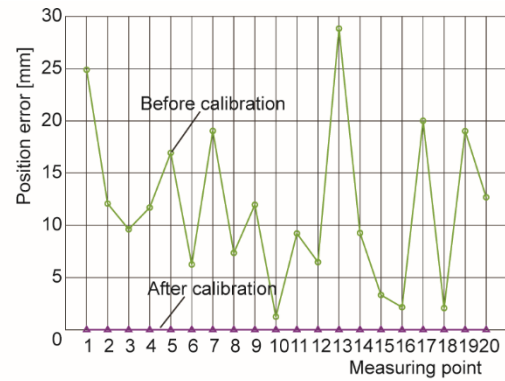


Figure 6. Adaptive ridge regression calibration results with redundant parameters removed

Table 3. Calibration results of the collaborative robot arm based on adaptive ridge regression

	Calibration results including all parameters				Calibration results with redundant parameters removed			
	Maximum error		Mean absolute error		Maximum error		Mean absolute error	
	Before	After	Before	After	Before	After	Before	After
$\Delta x$	4.1749	-0.00374	1.3808	0.0019	4.4971	0.001815	2.0510	0.00068843
$\Delta y$	-4.0525	-0.00397	1.8824	0.0019	3.5381	-0.00148	2.0157	0.0006591
$\Delta z$	2.9364	-0.00418	1.0735	0.0028	2.9364	-0.00148	1.2024	0.0005182
$\sqrt{\Delta x^2 + \Delta y^2 + \Delta z^2}$	22.2867	$2.154 \cdot 10^{-5}$	9.6469	$1.842 \cdot 10^{-5}$	28.8381	$3.582 \cdot 10^{-6}$	13.1706	$1.774 \cdot 10^{-6}$

The experimental results demonstrate that the iterative identification results of the least squares method are compromised when redundant parameters are not removed. This leads to significant end-effector positioning errors after calibration. This is due to the presence of numerous linearly related arrays in the identification Jacobian matrix, which results in a large condition number and model instability. Following the removal of redundant parameters, the identification and calibration accuracy of the least squares method exhibited a notable improvement, with the mean absolute error decreasing from 10.3727 mm to  $1.4907 \times 10^{-6}$  mm. The proposed iterative parameter identification method demonstrates efficacy even in the presence of redundant parameters, exhibiting enhanced generalization, stability, and robustness, as well as reduced overfitting. This is achieved through the automatic selection of regularization parameters, which enhances the model adaptability. The maximum calibration error decreased from 22.2867 mm to  $2.154 \times 10^{-5}$  mm, and the mean absolute error decreased from 9.6469 mm to  $1.842 \times 10^{-5}$  mm. Following the removal of redundant parameters, the calibration values are found to be approximately equal to those of the least squares method, thereby confirming the effectiveness of the redundancy elimination process. The maximum error decreased from 28.8381 mm to  $3.582 \times 10^{-6}$  mm, and the mean absolute error decreased from

13.1706 mm to  $1.774 \times 10^{-6}$  mm. In summary, the performance of the proposed method is superior to that of the least squares method.

## Conclusion

The study established a robot error model using the perturbation method and provided an analytical method for eliminating redundant parameters. The adaptive ridge regression iterative identification algorithm was employed to enhance the parameter identification and calibration of collaborative robots. The experimental results demonstrated that the least squares method was unable to achieve successful calibration outcomes when redundant parameters were not eliminated. The proposed iterative parameter identification method demonstrated satisfactory performance even in the presence of redundant parameters and exhibited a notable improvement in calibration accuracy following their removal. This validates the stability and robustness of the proposed method in addressing multicollinearity issues, demonstrating superior generalization capability and adaptability.

## Acknowledgment

The authors would like to thank the funding support to this research from the National Natural Science Foundation of China (Grant No. 52375517), the Key Projects of the National Natural Science Foundation of China (Grant No. 92067205), the Aeronautical Science Foundation of China (Grant No. 2018ZE53050).

## References

- [1] Wang, X. V., et al., Human-Robot Collaborative Assembly in Cyber-Physical Production: Classification Framework and Implementation, *CIRP annals*, 66 (2017), 1, pp. 5-8
- [2] Villani, V., et al., Survey on Human-Robot Collaboration in Industrial Settings: Safety, Intuitive Interfaces and Applications, *Mechatronics*, 55 (2018), Nov., pp. 248-266
- [3] Xuan, J., Sun, H. X., Review on Kinematics Calibration Technology of Serial Robots, *International Journal of Precision Engineering and Manufacturing*, 15 (2014), Aug., pp. 1759-1774
- [4] Zhang, T., et al., An Online Prediction and Compensation Method for Robot Position Errors Embedded with Error-Motion Correlation, *Measurement*, 234 (2024), 114866
- [5] Kang, M., et al., A Robot Positional Error Compensation Method Based on Improved Kriging Interpolation and Kronecker Products, *IEEE Transactions on Industrial Electronics*, 71 (2023), 4, pp. 3884-3893
- [6] Li, Z., et al., An Overview of Calibration Technology of Industrial Robots, *IEEE/CAA Journal of Automatica Sinica*, 8 (2021), 1, pp. 23-36
- [7] Denavit, J., Hartenberg, R. S., A Kinematic Notation for Lower-Pair Mechanisms Based on Matrices, *ASME Journal of Applied Mechanics*, 22 (1955), 2, pp. 215-221
- [8] Xiang, T., et al., Kinematics Parameter Calibration of Serial Industrial Robots Based on Partial Pose Measurement, *Mathematics*, 11 (2023), 23, 4802
- [9] Hayati, S. A., Robot Arm Geometric Link Parameter Estimation, *Proceedings*, 22<sup>nd</sup> IEEE Conference on Decision and Control, San Antonio, Tex., USA, 1983, pp. 1477-1483
- [10] Zhuang, H., et al., A Complete and Parametrically Continuous Kinematic Model for Robot Manipulators, *IEEE Transactions on Robotics and Automation*, 8 (2002), 4, pp. 451-463
- [11] He, J.-H., et al., A Local POE-Based Self-Calibration Method Using Position and Distance Constraints for Collaborative Robots, *Robotics and Computer-Integrated Manufacturing*, 86 (2024), 102685
- [12] Selingue, M., et al., Hybrid Calibration of Industrial Robot Considering Payload Variation, *Journal of Intelligent & Robotic Systems*, 109 (2023), 3, 58
- [13] Cheng, Y. B., et al., Small Sample Uncertainty Evaluation of Industrial Robot Position Accuracy Measurement Based on Grey Model, *Measurement Science and Technology*, 35 (2024), 8, 086006
- [14] Gao, G. B., et al., Modeling and Parameter Identification of a 3D Measurement System Based on Redundant Laser Range Sensors for Industrial Robots, *Sensors*, 23 (2023), 4, 1913
- [15] Khayat, F., Identification of Piecewise Constant Robin Coefficient for the Stokes Problem Using the Levenberg-Marquardt Method, *Computational and Applied Mathematics*, 39 (2020), June, pp. 1-23

- [16] Xu, X. K., et al., A Modeling and Calibration Method of Heavy-Duty Automated Fiber Placement Robot Considering Compliance and Joint-Dependent Errors, *Journal of Mechanisms and Robotics*, 15 (2023), 6, 061011
- [17] Toquica, J. S., Motta, J. M., A Novel Approach for Robot Calibration Based on Measurement Sub-Regions with Comparative Validation, *The International Journal of Advanced Manufacturing Technology*, 131 (2024), Aug., pp. 3995-4008
- [18] Deng, Y. H., et al., A Highly Powerful Calibration Method for Robotic Smoothing System Calibration via Using Adaptive Residual Extended Kalman Filter, *Robotics and Computer-Integrated Manufacturing*, 86 (2024), 102660
- [19] Lim, H. K., et al., A Practical Approach to Enhance Positioning Accuracy for Industrial Robots, *Proceedings, 2009 ICCAS-SICE*, Fukuoka, Japan, 2009, pp. 2268-2273
- [20] Li, R., et al., Real-Time Trajectory Position Error Compensation Technology of Industrial Robot, *Measurement*, 208 (2023), 112418
- [21] Hatami, M., et al., *Differential Transformation Method for Mechanical Engineering Problems*, Academic Press, New York, USA, 2017
- [22] Yun, H., et al., Calibration of Industrial Robots with Spherical Joint Using Single Wire Encoder, *Manuf Lett*, 33 (2022), Aug., pp. 46-50
- [23] Zhu, Q., et al., Kinematic Self-Calibration Method for Dual-Manipulators Based on Optical Axis Constraint, *IEEE Access*, 7 (2018), Dec., pp. 7768-7782